Geometric LPV Fault Detection Filter Design for Commercial Aircrafts

Bálint Vanek*† Zoltán Szabó * András Edelmayer ‡

József Bokor §

Computer and Automation Research Institute Hungarian Academy of Sciences, Budapest, Hungary.

The present paper applies the geometric linear parameter-varying (LPV) fault detection methods to a high-fidelity commercial aircraft problem. The successive steps of the design, including fault modeling, LPV model generation, and LPV FDI filter synthesis are discussed. Geometric fault detection and isolation filters are known for having excellent fault isolation, fault reconstruction and sensitivity properties under small modeling uncertainty and noise. However they are assumed to be sensitive to model uncertainty and noise, hence an investigation is made to assess the robustness properties of the proposed design framework. The novelty of the present paper is in the application of robust post-filtering of the raw LPV fault detection residual, by applying an $\mathcal{H}_\infty$ output injection gain to the nominal fault detection filter. To asses the performance of the geometric filter, an aircraft dynamics example is presented, where aileron actuator faults are detected and isolated from additional elevator and rudder fault cases.

I. Introduction

Modern fly-by-wire aircraft flight control systems are becoming more complex with many actuators controlling several aerodynamic surfaces. While performance goals, including aerodynamic drag minimization and structural load suppression are becoming more and more important, flight must be kept at the same highest safety level. In parallel, there is a clear trend towards the All-Electric Aircraft. Recently, Airbus introduced on the A380 a new hydraulics layout [20], where the three Hydraulics circuitry is replaced by a two Hydraulics plus two Electric layout, which saves one ton mass for the aircraft. Each primary surface has a single hydraulically powered actuator and electrically powered back-up with the exception of the outer aileron, which uses the two hydraulic systems together. Consequently, the trends of complexity and more-electric architectures, like Electromechanical Actuators (EMA) with more fault sources, raise the importance of availability, reliability and operating safety. For safety critical systems, like aircraft, the consequence of faults in the control system hardware and software can be extremely serious in terms of human mortality and economical impact. This is the reason why all aircraft manufacturers are compliant with stringent safety regulations of FAA, EASA and other aviation authorities. However, there is a growing need for on-line supervision and fault diagnosis to satisfy the newer societal imperatives towards an environmentally-friendlier aircraft with still the highest level of safety and reliability. The traditional approach to fault diagnosis in the wider application context is based on hardware redundancy methods which use multiple sensors, actuators computers and software to measure and control a particular variable [10]. Based on the mathematical model of the plant, analytical relation between different sensor outputs can be used to generate residual signals. There is a growing interest in methods which do not require additional hardware redundancy, and only rely on the ever increasing level of computational power onboard the aircraft.

In analytical redundancy schemes, the resulting difference generated from the consistency checking of different variables is called as a residual signal. The residual should be zero when the system is normal, and should diverge from zero when a fault occurs in the system. This zero and non-zero property of the

*senior research fellow, Systems and Control Laboratory
†corresponding author:vanek@sztaki.hu
‡research advisor, Systems and Control Laboratory
§research director, Head of Systems and Control Laboratory

residual is used to determine whether or not faults have occurred. Analytical redundancy makes use of a mathematical model and the goal is the determination of faults of a system from the comparison of available system measurements with a priori information represented by the mathematical model, through generation of residual quantities and their analysis. Various approaches have been applied to the residual generation problem, the parity space approach [6], the multiple model method [4], detection filter design using geometric approach [14], frequency domain concepts [9], unknown input observer concept [5], dynamic inversion based detection [8], and using rational nullspace bases [22]. Most of these design approaches refer to linear time-invariant (LTI) systems. The geometric concept is further generalized to linear parameter-varying (LPV) systems by [1], while input affine nonlinear systems are considered by [7]. The basic concepts underlying observer-based fault detection and isolation (FDI) schemes are the generation of residuals and the use of an optimal or adaptive threshold function to differentiate faults from disturbances, see the surveys of [9, 16]. Generally, the residuals, also known as diagnostic signals, are generated by the FDI filter from the available input and output measurements of the monitored system. The threshold function is used to robustify the detection of the fault by minimizing the effects from false faults, disturbances and commands on the residuals. For fault isolation, the generated residual has to include enough information to differentiate said fault from another, usually this is accomplished through structured residuals or directional vectors. Robustness of the FDI algorithm is determined by its capability to decouple the filter performance outputs from disturbances, errors, and unmodelled dynamics.

The geometric design approach, for example, is known for its excellent fault isolation, fault reconstruction and sensitivity properties under small modeling uncertainty and noise. This paper shows the application of the geometric LPV FDI approach to a complex, 6-degrees-of-freedom (DOF) rigid body aircraft model. Previous approaches [19, 13] only considered the longitudinal dynamics of the airplane, which is applicable for elevator fault detection case but as described in [21] designs based on decoupled dynamics are inherently limited to detection around the trim (cruise) flight condition and might be less robust to deviation from the trim operating point. One possible extension of the geometric LPV FDI approach is to take advantage of the possible multi dimensional residual signal. The output of the geometric FDI filter spans the entire subspace where the fundamental problem of residual generation (FPRG) has a solution. Only ad-hoc methods have been described in the literature to form a proper residual signal based on a subset of the geometric FDI filter outputs. In the present paper the entire subspace spanned by multiple outputs are used to form a residual signal, which provides improved fault reconstruction an fault detection response performance, together with improved robustness, which is explicitly handled by the post-filter synthesis.

Derivation of the LPV mathematical model, representing the aircraft dynamics and the effects of various actuator faults is discussed first. A geometric filter is designed on the nominal LPV plant, which only represents the rigid body states. The robustness of the geometric filter over the set of uncertain plants is analyzed to assess the applicability of the approach to the full nonlinear problem. The proposed filter is than analyzed on an augmented LPV model of the aircraft, which includes actuator and sensor dynamics. Finally, an aircraft aileron FDI example is detailed in the article with high-fidelity simulation results.

The importance of this paper is on the application (simulation) of the geometric approach based LPV FDI technique to a nonlinear, high-fidelity 6-DOF aircraft simulator, where issues of model uncertainty, realistic disturbances and robustness have to be accounted for in the design stage. The remainder of the paper is structured as follows. Section II and III presents the notation and basic concepts of geometric fault detection filter design. The application example of a civil aircraft is described in Section IV. The method is applied to the high fidelity aircraft example, which demonstrates the proposed approach, given in Section V. Finally, the paper is concluded in Section VI.

II. Notation

$\mathbb{R}$ and $\mathbb{C}$ denote the set of real and complex numbers, respectively. $\mathbb{RH}_\infty$ denotes the set of proper, rational functions with real coefficients that are analytic in the closed right half of the complex plane. $\mathbb{R}^{m\times n}$, $\mathbb{C}^{m\times n}$, and $\mathbb{RH}_\infty^{m\times n}$ denote the sets of $m \times n$ matrices whose elements are in $\mathbb{R}$, $\mathbb{C}$, and $\mathbb{RH}_\infty$, respectively. A single superscript index is used to denote vectors, e.g. $\mathbb{R}^l$ denotes the set of $l \times 1$ vectors whose elements are in $\mathbb{R}$. For a matrix $M \in \mathbb{C}^{m\times n}$, M^* denotes the complex conjugate transpose. $\bar{\sigma}(M)$ and $\underline{\sigma}(M)$ denote the maximum and minimum singular values. $\|M\|$ denotes the matrix norm induced by the vector 2-norm. It is known that $\|M\| = \bar{\sigma}(M)$. For a vector $v \in \mathbb{C}^n$, $Re[v]$ denotes the real part of v. For $G \in \mathbb{RH}_\infty^{m\times n}$, $\|G\|_\infty := \sup_\omega \bar{\sigma}(G(j\omega))$. Finally, let $G \in \mathbb{RH}_\infty^{(n+k)\times(n+m)}$ and $\Delta \in \mathbb{RH}_\infty^{n\times n}$ be given

and partition $G := \left[\begin{smallmatrix} G_{11} & G_{12} \\ G_{21} & G_{22} \end{smallmatrix}\right]$ with $G_{11} \in \mathbb{RH}_\infty^{n\times n}$ and $G_{22} \in \mathbb{RH}_\infty^{k\times m}$. If $I - G_{11}\Delta$ is invertible at $\omega = \infty$, then define $F_u(G, \Delta)$ as the linear fractional transformation (LFT) obtained by closing Δ around the upper channels of G:

$$F_u(G, \Delta) := G_{22} + G_{21}\Delta \left(I - G_{11}\Delta\right)^{-1} G_{12} \tag{1}$$

III. Geometric FDI Filters for qLPV systems

This section briefly describes the formulation of fault detection filters designed using geometric concepts. The derivation of the geometric FDI filters is presented for qLPV systems with no disturbance, no uncertainty and the detection and isolation of two faults. Consider the qLPV system with two additive actuator faults:

$$\begin{aligned} \dot{x} &= A(\rho)x + B(\rho)u + L_1(\rho)f_1 + L_2(\rho)f_2 \\ y &= Cx \end{aligned} \tag{2}$$

where L_1 and L_2 represent the faults directions in the state space. f_1 and f_2 are the fault signals. The time varying scheduling parameter ρ is assumed to be available at operational time.

The fault signals are zero if there is no fault but nonzero if the particular fault occurs. Only actuator faults are considered here but sensor faults can also be considered within the theory. The fundamental problem of residual generation is to synthesize residual generators (filters) with outputs r_i $(i = 1, 2)$ that have the following decoupling property: r_i is sensitive to f_i but insensitive to f_j, $i \neq j$. More precisely, if $f_i = 0$ then $\lim_{t\to\infty} r_i(t) = 0$ and if $f_i \neq 0$ then $r_i \neq 0$.

The solution of this problem depends on the parameter varying (C, A)-invariant subspaces and certain parameter varying unobservability subspaces [1]. A parameter varying (C, A)-unobservability subspace $\mathcal{S}$ is a subspace such that there exist matrices $G(\rho)$ and H with the property that $\mathcal{S}$ is the maximal parameter varying $(A + GC)$ invariant subspace contained in Ker HC. The family of parameter varying (C, A)-unobservability subspaces containing a given set $\mathcal{L}$ has a minimal element. Define $\mathcal{L}_i = \text{Im } L_i$ $(i = 1, 2)$ and denote by $\mathcal{S}^*$ the smallest parameter varying unobservability subspace containing $\mathcal{L}_2$. Then the fundamental problem of residual generation has a solution if and only if $\mathcal{S}^* \cap \mathcal{L}_1 = 0$ [15, 2]. The condition $\mathcal{S}^* \cap \mathcal{L}_1 = 0$ ensures that the fault to be detected is not hidden in the parameter varying unobservability subspace of the detection filter. In fact, the fault direction will be decoupled from the rest of the fault directions since they are contained in the parameter varying unobservability subspace of the residual generator.

The residual generator associated with fault direction L_1 can be described by an observer of the form:

$$\begin{aligned} \dot{w} &= N(\rho)w - G(\rho)y + F(\rho)u \\ r_1 &= Mw - Hy \end{aligned} \tag{3}$$

where u and y are the known input and measured output signals of the original qLPV system. w is the state of the residual generator and r_1 is the residual.

Denote by P the projection operator $P : \mathcal{X} \to \mathcal{X}/\mathcal{S}^*$. The state matrices can be determined as follows [3]. H is a solution of the equation Ker $HC =$ Ker $C + \mathcal{S}^*$, and M is the unique solution of $MP = HC$. Consider a gain matrix $\hat{G}$ chosen such that $(A + \hat{G}C)\mathcal{S}^* \subseteq \mathcal{S}^*$ and define $\hat{A} = P(A + GC)P^T$. $\hat{A}$ does not necessarily define a stable system. To obtain quadratically stable filters one can set $N = \hat{A} + \tilde{G}M$, where $\tilde{G} := X^{-1}K$ and X, K are determined from the linear matrix inequality (LMI):

$$0 \succeq \hat{A}^T(\rho)X + X\hat{A}(\rho) + M^T K^T(\rho) + K(\rho)M \tag{4}$$

$$0 \preceq X = X^T, \tag{5}$$

for every parameter ρ in the parameter space. Then set $G = P\hat{G} + \tilde{G}H$ and $F = PB$.

If the parameter dependence of the time varying scheduling variables is affine, then the relevant parameter varying invariant subspaces can be computed and the set of LMIs can be solved. Using this approach there are as many filters as faults to detect, and their state dimensions are equal to the dimension of $\mathcal{X}/\mathcal{S}^*$. The filter gains can be tuned in order to impose robustness properties to the detection filter.

A. Robust FDI filter for Model Matching

Since the geometric LPV FDI design does not consider model uncertainty, the detection performance has to be robustified by additional methods. It is shown in [17] that filter synthesis for uncertain plants using the

model matching framework has a self-optimality property, leading to fault detection performance which is robust. The framework of [17] is extended here to address the special properties of geometric FDI filters with multi-dimensional residual subspaces. The filter dynamics described in Eq. 3 can be shaped by appropriate output injection, using $N(\rho) = A_0(\rho) + D_1(\rho)M$ the poles of the filter can be assigned arbitrarily. Since the output r_1 of the FPRG filter spans the whole subspace which satisfies the FPRG problem, an FDI post-filter acting on these signals does not change the fault decoupling and isolating properties of the original scheme, it just shapes the fault detection response. The post-filter employed here assigns the dynamics of $N(\rho)$ in a way, fault reconstruction is satisfied on the uncertain plant using the model matching framework, with ideal behavior T_{id}, as shown in Figure 1.

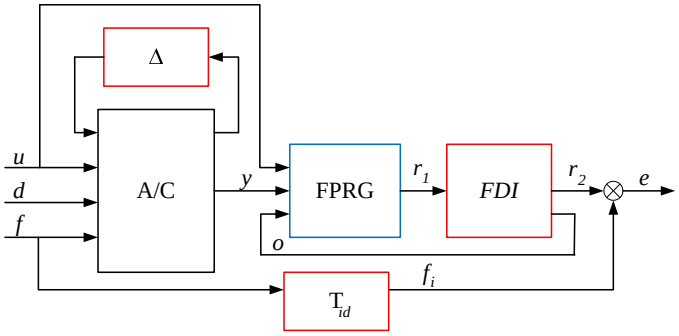

Figure 1. Framework for robust model matching FDI filter synthesis .

IV. Aircraft Model

A. General Aircraft Characteristics

The aircraft model used in the project is an aircraft from Airbus. The aircraft has two engines and its nominal configuration, along with the operation range considered in the project, is listed in Table 1. The

Table 1. System parameters of the A/C model

Parameter	Description	Value and Units	Uncertain bounds
m	Weight,	200 tonns	[180;220]
h	Altitude,	37000 ft	[15000;40000]
CG	position of c.g. rel. to mean aero. chord,	0.3	[0.27;0.33]
V_{cas}	Calibrated airspeed,	267 kts	[160;320]

aircraft has 18 control inputs (since airbrake is not effective in cruise flight, it is removed from the list of inputs), and measurement of 6-DOF motion with load factor (n_x, n_y, n_z), body rate (p, q, r), velocity (V_T), aerodynamic angles (α, β), position (X, Y, Z) and attitude (ϕ, θ, ψ) outputs. The inputs are listed in Table 2: Notice that Trimmable Horizontal Stabilizer is used for longitudinal trimming purposes, elevator deflections are zero. Since cruise flight condition is symmetric, none of the ailerons, spoilers or the rudder are deflected to provide trim.

The rigid body aircraft equations of motion are augmented with nonlinear actuator [11] and sensor characteristics. The nonlinear body-axes rigid body dynamics includes 13 states using quaternion formalism: p, q, r body rates, u, v, w velocities all in body axes, q_0, q_1, q_2, q_3 quaternions, representing the rotation between the body and inertial axes, and X, Y, Z positions in the North-East-Down coordinate frame, assuming Flat Earth for simplicity.

Table 2. System inputs of the A/C model

Input	Description	Trim Value and Units
$pi1$	Left Engine Throttle,	1.2235 deg
$pi2$	Right Engine Throttle,	1.2235 deg
$\delta_{a,IL}$	Aileron internal Left,	0 deg
$\delta_{a,IR}$	Aileron internal Right,	0 deg
$\delta_{a,EL}$	Aileron external Left,	0 deg
$\delta_{a,ER}$	Aileron external Right,	0 deg
$\delta_{sp,1L}$	Spoiler 1 Left,	0 deg
$\delta_{sp,1R}$	Spoiler 1 Right,	0 deg
$\delta_{sp,23L}$	Spoiler 2, 3 Left,	0 deg
$\delta_{sp,23R}$	Spoiler 2, 3 Right,	0 deg
$\delta_{sp,45L}$	Spoiler 4, 5 Left,	0 deg
$\delta_{sp,45R}$	Spoiler 4, 5 Right,	0 deg
$\delta_{sp,6L}$	Spoiler 6 Left,	0 deg
$\delta_{sp,6R}$	Spoiler 6 Right,	0 deg
$\delta_{e,L}$	Elevator Left,	0 deg
$\delta_{e,R}$	Elevator Right,	0 deg
δ_r	Rudder,	0 deg
δ_{ih}	Trimmable Horizontal Stabilizer,	-2.3939 deg

B. Deriving a reliable LPV model

The ADDSAFE benchmark model of the aircraft is given in a nonlinear simulation, where several components are given as black-box models. Aerodynamic coefficients are represented by trained neural-networks, for which it is not possible to derive affine LPV models in the form of Equation 2 analyticaly.

On the basis of the required operating envelope it is decided to have weight, center of gravity position, altitude above sea level, and calibrated airspeed as scheduling variables. The nonlinear model is then trimmed and linearized at different points of the operating envelope to obtain pointwise LTI models. These LTI models are then approximated by an affine LPV model using the DLR propriatary LFR toolbox. The procedure is described in detail in [12].

When obtaining the LPV representation, several simplifying assumptions are made to reduce the problem size. The airbrake, which is disabled at high Mach numbers, is removed from the control inputs since it has no effect on the aircraft. Since the original aircraft model uses quaternions, which impose additional constraints on the state equations, the model used for trim, linearization and LPV model generation is rewritten using conventional Euler angles [18]. The LPV model is open-loop, without the control loop and, since the actuators and sensors are assumed to have unit steady state gain and low-pass characteristics, their dynamics are omitted. Trim is obtained with zero aileron, rudder and elevator deflection, left and right engines are providing the same amount of thrust to balance the yawing motion. Pitch axis trim is obtained with the Trimmable Horizontal Stabilizer, while the aircraft has constant (parameter depending) Angle-of-attack. Since the resulting 12 state linear model is unstable additional simplifications have to be done. The open loop aircraft model is slightly unstable around the yaw angle (ψ), and has two modes (X, Y) which are integrators. Since the FDI problem is invariant of X, Y positions and yaw angle these states are removed from the dynamics, truncating these states does not change the dynamics of the remaining states. The resulting model with nine states, as described in [21], almost perfectly matches the original 12 states model, and stable in the behavior of the remaining states, and outputs in a limited flight envelope. The flight envelope in the current investigation spans the following space: $h = [23000; 29000]ft$, $V_{cas} = [170; 230]kts$, while cg. position is fixed to $x_{cg} = 0.3$ and weight is also assumed constant with $m = 200000kg$. The LPV model has two scheduling parameters $\rho = (h, V_{cas})$, this simplification is necessary to obtain computationaly tractable problems. The final rigid body LPV model, assuming full state measurement, is obtained in a form

of:

$$\dot{x} = (A_0 + A_h h + A_V V)x + (B_0 + B_h h + B_V V)u + (F1_0 + F1_h h + F1_V V)f_1 + (F2_0 + F2_h h + F2_V V)f_2 \tag{6}$$

$$y = x$$

The engine, sensor and actuator models are not studied in the current investigation, only the rigid body dynamics are approximated by the LPV model. When the nonlinear aircraft characteristics have to be compared to the behavior of the corresponding LPV A/C model the schematics used in Figure 2 should be used.

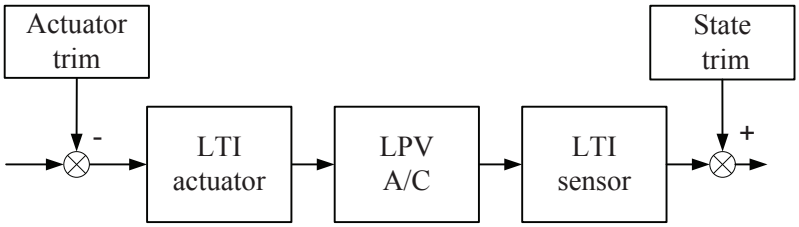

Figure 2. Interconnection of the LPV rigid body equations with sensor and actuator model.

The resulting LPV model can be augmented with first order sensor and actuator dynamics derived from the high-fidelity simulation, to account for their effect on the aircraft behavior. Since the filters obtained by geometrical FDI methods require intense computation onboard the aircraft, only the pure rigid body dynamics model will be investigated for filter synthesis first.

C. Actuator Fault Model

The fault scenario under investigation is left inboard aileron fault. To account for the various types of faults the original affine LPV system description of have to be augmented with additional fault directions as in Equation 2.

$$\dot{x}(t) = A(\rho(t))x(t) + B(\rho(t))u(t) + L_1(\rho(t))f_{a,i,L}(t) + L_2(\rho(t))f_{e,L}(t) + L_3(\rho(t))f_r(t) \tag{7}$$

$$\tilde{y}(t) = \tilde{C}x(t) \tag{8}$$

Where $L_1(\rho(t)) = B(3,:)(\rho(t))$ is the corresponding column of the control effectiveness matrix of the left inboard aileron. $L_2(\rho(t)) = B(14,:)(\rho(t))$ corresponds to the left elevator control effectiveness, while $L_3(\rho(t)) = B(16,:)(\rho(t))$ is the column of the rudder control effectiveness, in addition to fault directions, the effect of the unknown wind disturbance is also included in the system model by additional columns in the $B(\rho(t))$ matrix. One can attempt to design an FDI filter which is insensitive not only for elevator and rudder faults, but also insensitive for the w_x, w_y, w_z components of winndgust. It is important to note, that although we are interested in detecting left internal aileron faults we included the effect of additional actuator faults. It is necessary, since in the design stage we want to design an FDI filter which is sensitive for faults in the direction of L_1, but to provide good isolation and to keep false alarm rate low the filter should be insensitive for additional faults characterized by the directions of L_2 and L_3. On the other hand, adding additional actuators to the augmented plant does not provide additional benefits, since the right aileron has exactly the same B matrix with an opposite sign, hence these two faults lie in the same subspace. The outer ailerons are creating similar effect on the aircraft and are virtually indistinguishable from the inner ailerons if the system becomes uncertain. The left and the right elevator have also the same column in their control effectiveness matrix. While engines have significantly slower dynamics and their diagnostics is well established. While fault of a single spoiler creates significantly smaller response than the primary control surfaces, hence in the initial investigation they are omitted.

It is also interesting to note, that only a subset of sensor measurement outputs $\tilde{y}$ are selected by $\tilde{C}$ for the fault detection problem. Namely, the measurement of acceleration is omitted, since actuator inputs have

direct feedthrough and hence their D matrix is nonzero, which is difficult to handle in the geometric FDI framework.

The various fault scenarios to be investigated are disconnection, stuck and bias on the aileron actuator. In case of disconnection, the aileron surface goes to the position dictated by the aerodynamic forces acting on it, which is at -12 deg, the physical limit on the deflection. The failure signal is defined as $f_{a,i,L}(t) = -12deg - u_{a,i,L}(t)$. The other scenario is liquid jamming, when a bias $b_{l,j}$ occurs on the rod sensor, and hence on the rod position relative to the commanded deflection. This can be captured by a fault signal of $f_{a,i,L}(t) = b_{l,j}$. The third case is called solid jamming, when the actuator is stuck at a given position $b_{s,j}$ and does not move, this is similar to the first scenario, only the offset is not 12 degrees but some other quantity $b_{s,j}$.

V. FDI Filter Design for the Aircraft

A geometric LTI FDI filter is designed first for the aileron fault detection problem of the aircraft. In the linear case it is possible to design a filter which decouples aileron faults from elevator, rudder faults and windgust disturbances. First, the filter design steps are detailed and the achieved performance is analysed. Detailed simulations on the high-fidelity aircraft model with injected faults follows.

A. Filter Design Steps

The main idea behind the filter design formulation is that aileron faults appear on the filter residual output, while elevator and rudder faults are embedded in the unobservability subspace of the filter. For that reason the the nominal design point of the LPV model derived in Section IV, with additional windgust disturbance inputs, is augmented with left inner aileron, left elevator, and rudder faults, by using the successive input directions from the $B(\rho)$ and $D(\rho)$ matrices as fault directions in the linear model. Load factor, n_x, n_y, and n_z, measurement is omitted from the model, since the $D(\rho)$ matrix associated with these acceleration outputs is nonzero, which makes the geometric FDI synthesis more complicated. The resulting LTI FPRG filter, using the methods developed in [2], has 6 residual output, 27 inputs, and 6 states. Since perfect decoupling is possible, the transfer functions between elevator to residual and rudder to residual are zero, while the 6 residual signals have different tracking responses for aileron faults.

To enhance the performance of the obtained filter, the LTI aircraft model is augmented with first order sensor and actuator models, on all input and output channels. Since the corresponding mathematical models are Airbus propriety, they are not discusses here. Using the schematics of Figure 1 the model matching problem is set up, with $T_{id} = \frac{s^2}{s^2+2s+1}$, where the problem is to find the $\mathcal{H}_\infty$ optimal filter FDI which has 6 inputs from the nominal geometric filter FPRG and provides 7 outputs, 6 of which are fed back to the FPRG filter using output injection, while the 7th output of the filter is used to form a residual. The residual is penalized to match the ideal behavior of T_{id} in the design framework. Note, that it is desirable to have actuator and sensor dynamics included in the FPRG filter design, which is not the case here since computational complexity of those filters are significantly higher.

Based on the design experience gained in the linear FPRG synthesis, the LPV fault detection filter design is solved next. Since decoupling aileron faults, from all additional disturbances, including elevator, rudder faults and windgust, is not feasible, a subset including only elevator faults is used in the LPV FPRG design. The resulting LPV FPRG filter has 4 states and 4 outputs, with zero gain from elevator faults and different responses from aileron faults on all 4 outputs. The performance of the LPV FPRG filter is also enhanced by a post-filter. For simplicity reasons the FDI post-filter design is based on the nominal LTI plant of the LPV model. Similarly to the previous case, the aircraft model is augmented with actuator and sensor dynamics, and the 4 outputs of the FPRG filter are used as measurements in the FDI post-filter, where 4 out of the 5 outputs are used for output injection to change the dynamics of the FPRG filter, while the fifth is used to form a residual. The residual is penalized to match the ideal behavior of T_{id} in the design framework.

B. Simulation Results

The filters are applied to the nonlinear aircraft model after taking the trim values into consideration, on both control input and sensor output signals. Since the simulation is implemented under SIMULINK with $0.01sec$ fixed step size, the corresponding filters are also discretized with the same sampling time using bilinear transformation. It is also worth mentioning, that the simulation is in closed-loop with the flight

control system set to altitude and heading hold mode and moderate atmospheric windgust disturbances are perturbing the aircraft flight. It is important to note the implementation of the LPV FDI filter, where the trim conditions on both input and output side have to be scheduled with the flight condition.

To be able to establish the thresholds on fault detection, to have low false alarm rate, while as few as possible missed detections the filter performance is analyzed in fault free situations first. It is seen in initial investigations, that a transient response occurs at the simulation start, which is due to the unexpected behavior of the control system, hence simulation plots only show responses from $10s$ after the initial transient settles. Since the residual signal is very close to zero in fault free situations, the additional disturbance of elevator faults is used to set the minimum detection threshold. The excellent decoupling performance of the filters for elevator runaway faults is investigated, as shown in Figure 3. The left elevator starts to drift from its commanded position with 5 deg/s rate starting at 20 s. The simulation starts from the nominal flight condition of $200knots$ and $26000ft$, while cg position is set to $x_{cg} = 0.3$ and weight is $200000kg$.

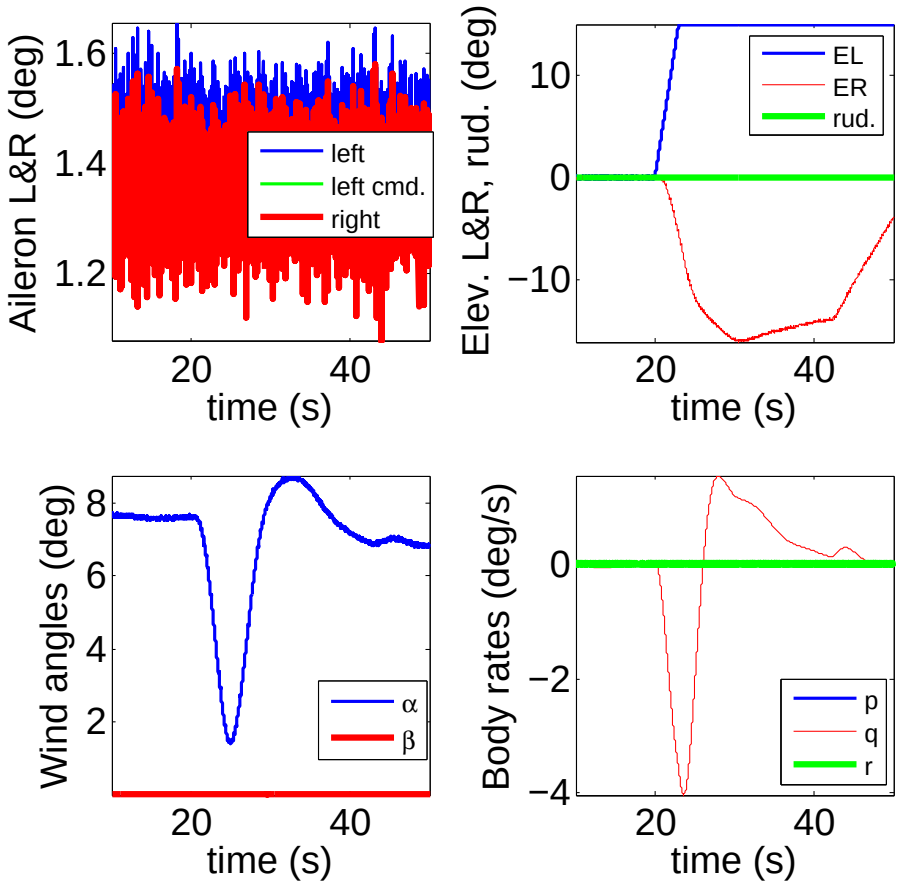

Figure 3. Left elevator runaway scenario, fault occurs at $20s$**.**

As seen on Figure 3 the fault creates significant pitch rate response and the angle of attack also changes dramatically during the maneuver, which leads to covering large part of the flight envelope. The right elevator with lower response time and later the THS compensates against the failure effect.

An increase in the residual signal can be seen in Figure 4. The LTI FDI residual reaches 0.175 deg expected aileron fault offset which is due to deviation from the trim flight condition, where the linear model used in the FDI filter design is no more accurate. The LPV FDI residual reaches a significantly lower value of 0.105 deg, which is due to the better mathematical model used in the LPV filter synthesis. Based on these results, where the elevator runaway can be regarded as a worst case disturbance, the detection thresholds are selected as 0.105×1.5 deg and 0.175×1.5 deg respectively for the LTI and LPV case. It is expected that in most situations, where aileron fault is not present, the residual signal stays away from the detection threshold, and as soon as the aircraft motion is stabilized the residual goes back to near zero value, avoiding triggering false alarms in the detection system.

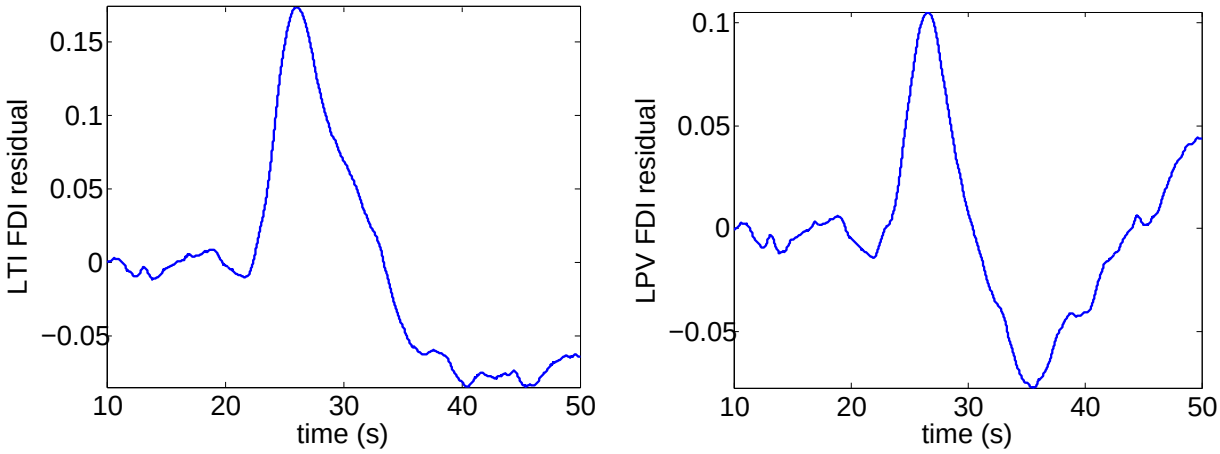

Figure 4. Left elevator runaway, LTI (left) and LPV (right) FDI filter residual.

After selection of the detection threshold the fault detection performance can be analyzed. The first aileron fault scenario is left inboard aileron disconnection as seen on Figure 5, this occurs when the connection between the actuator rod and the control surface is lost due to mechanical separation of the two components. Due to the aerodynamic forces, the freely floating aileron goes to $-12\ deg$ where it is reaching its physical limit, while the commanded position still remains positive as seen on Figure 5. The simulation starts from the nominal flight condition of $200knots$ and $26000ft$, while cg position is set to $x_{cg} = 0.3$ and weight is $200000kg$. The large unintended deflection leads to significant deviation from trim condition and the flight controller tries to compensate against it mainly in the lateral channel with rudder and right aileron, while the elevator commands are not influenced (see Fig.5). Significant sideslip can be seen also, which is due to asymmetric aircraft configuration, while roll rate has almost 3 deg/s peak after the fault occurs. Since this fault creates large roll rate and sideslip motion, which also leads to significant structural stress in the wings the detection of this fault is critical. Figure 6 shows a detection time of $0.51s$ in the LTI and $0.42s$ in the LPV case. The difference between the two detection times is mainly due to the difference in thresholds. It can be inferred from this result, that the performance of the LTI FDI approach is almost as good as the LPV, while it is significantly easier to implement the linear detection filter.

The most demanding fault scenario is left inboard aileron liquid jamming as seen on Figure 7, this means that a bias occurs on the rod sensor and the actuator shifts from it nominal $1.5deg$ deflection to $-0.75deg$ deflection and it remains $-2.25deg$ apart from it commanded position. To asses the performance difference, and the applicability of the LPV approach to a larger flight envelope, the simulation starts off from the nominal flight condition, from $170knots$ and $23000ft$, while cg position is set to $x_{cg} = 0.3$ and weight is $200000kg$. The operating envelope is explored in this maneuver since it is one of the corner points of the LPV model.

Figure 7 also shows the abrupt change in roll rate at $20sec$ when the fault occurs, otherwise slight deflection can be seen on the rudder but elevator and THS is unaffected, mainly the right aileron compensates the effect of the failure, which is much smaller and hence harder to detect than the disconnection. Using the above mentioned threshold a detection time of $0.87s$ is achieved with the LTI approach and $0.61s$ with the LPV method. What is worth to notice is the large difference between the steady state values of residuals. While both the LTI and the LPV filter are able to reconstruct the fault magnitude in the disconnection case, around the nominal flight condition, the reconstruction performance of the LTI filter in the off-nominal situation with small faults is compromised, as shown on Figure 8. On the other hand, the performance of the LPV FDI filter is excellent, only the initial transient has to be settled.

VI. Conclusions

This paper considers the design of geometric fault detection filters and their application to a high fidelity aircraft model, and shows the advantages of advanced model-based LPV methods which are, compared with

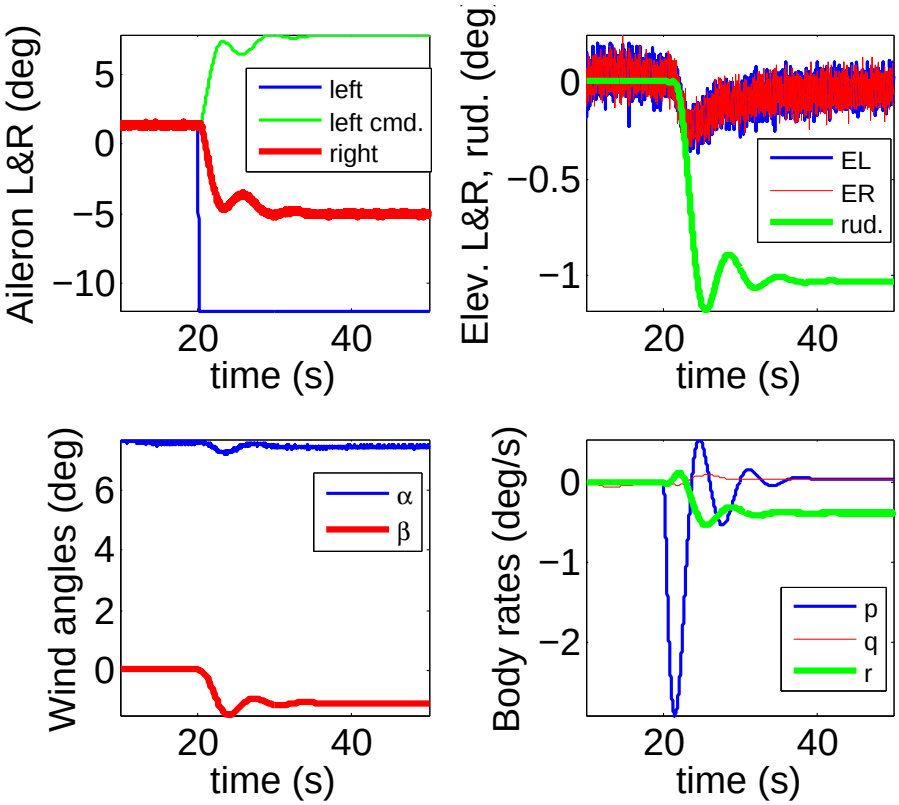

Figure 5. Left aileron disconnection scenario, fault occurs at $25s$.

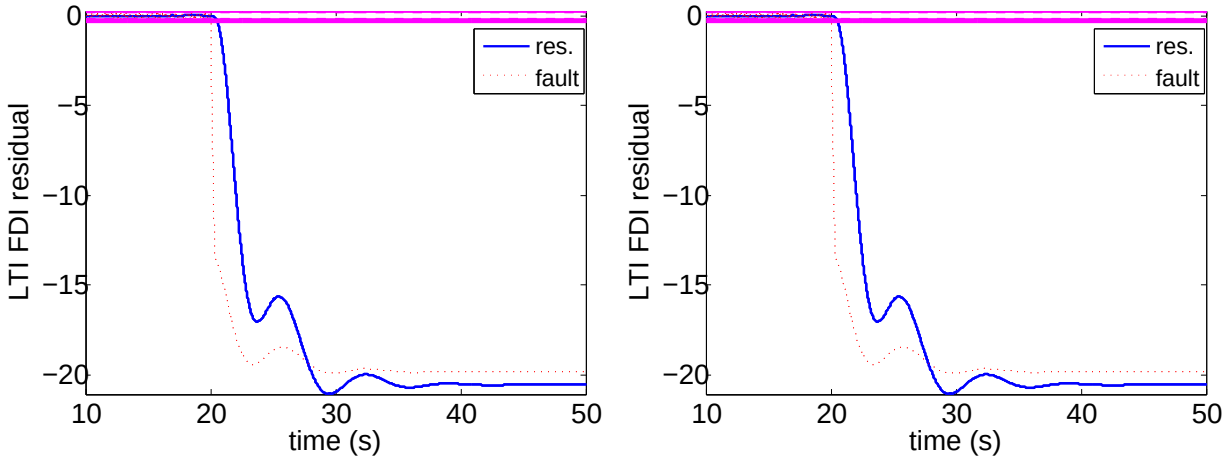

Figure 6. Left aileron disconnection, geometric FDI filter residual.

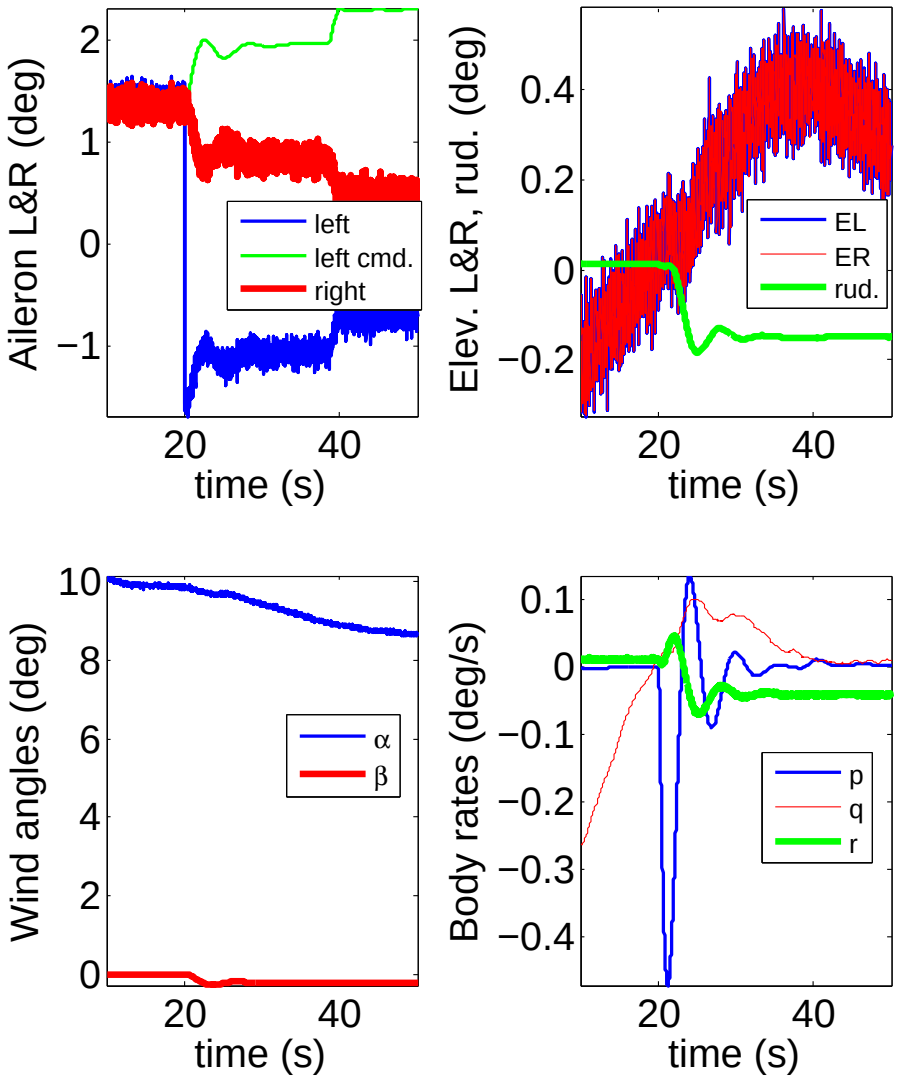

Figure 7. Left aileron liquid jamming scenario, fault occurs at $25s$.

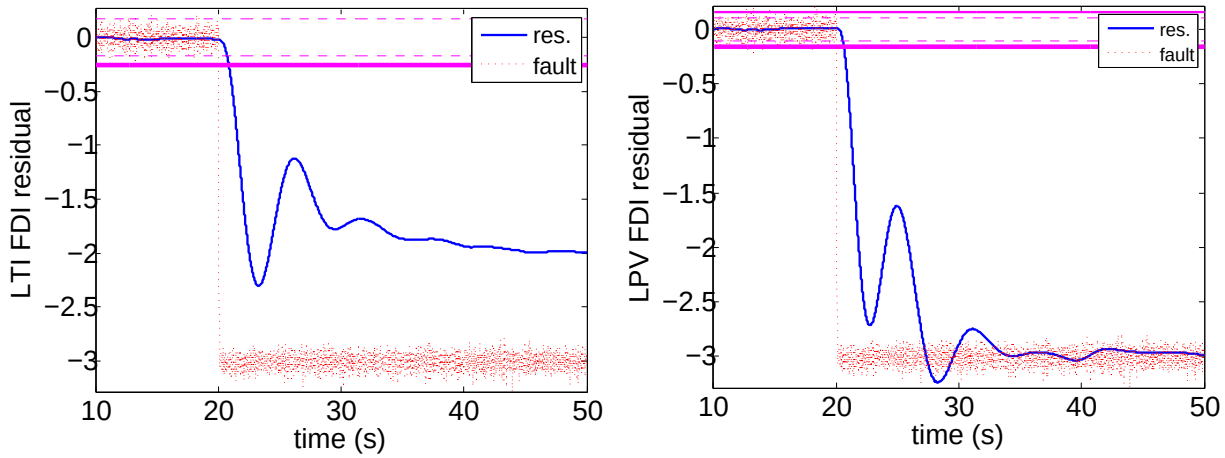

Figure 8. Aileron liquid jamming, LTI (left) and LPV (right) FDI filter residual.

the traditional LTI methods, applicable to a larger flight domain and hence in the future might be tested on industrial platforms. First, a geometric filter is designed on the nominal plant. Next the robustness of the proposed filter is enhanced on an uncertain aircraft model, using the robust model matching $\mathcal{H}_\infty$ problem formulation with appropriately chosen output injection. The proposed LPV filter is then applied to a high-fidelity aircraft model, where different aileron faults are successfully detected and when designed properly isolated from elevator faults in reasonable time. Further research should extend the validity of the present approach and based on the present findings provide a fault detection approach suitable for industrial test purposes.

VII. Acknowledgment

This work is supported by the ADDSAFE (Advanced Fault Diagnosis for Safer Flight Guidance and Control) EU FP7 project, Grant Agreement: 233815, Coordinator: Dr. Andrés Marcos. The authors are grateful for the discussions on FDI related problems with Gary Balas and Peter Seiler.

References

[1] G. Balas, J. Bokor, and Z. Szabo. Invariant subspaces for LPV systems and their applications. *IEEE Transactions on Automatic Control*, 48(11):2065–2069, 2003.

[2] J. Bokor and G. Balas. Detection filter design for LPV systems - a geometric approach. *Automatica*, 40:511–518, 2004.

[3] J. Bokor, Z. Szabo, and G. Stikkel. Failure detection for quasi LPV systems. In *Proceedings of the 41st IEEE Conference on Decision and Control (CDC'02), Las Vegas, NV, USA*, pages 3318–3323, 2002.

[4] C. B. Chang and M. Athans. State estimation for discrete systems with switching parameters. *IEEE Transactions on Aerospace and Electronic Systems*, 14:418–425, 1978.

[5] J. Chen and R. J. Patton. *Robust Model-based Fault Diagnosis for Dynamic Systems*. Kluwer Academic. Boston., 1999.

[6] E.Y. Chow and A.S. Willsky. Analytical redundancy and the design of robust failure detection systems. *IEEE Trans. on Automatic Control*, 29(7):603–614, 1984.

[7] C. De Persis, R. De Santis, and A. Isidori. Nonlinear actuator fault detection and isolation for a VTOL aircraft. In *Proceedings of the 2001 American Control Conference, Vols 1-6*, pages 4449–4454, 2001.

[8] A. Edelmayer, J. Bokor, and Z. Szabo. A geometric view on inversion-based detection filter design in nonlinear systems. In *Proceedings of the 5th IFAC symposium on fault detection, supervision and safety of technical processes. SAFEPROCESS 2003, Washington*, pages 783–788, Washington, 2003.

[9] P.M Frank. Fault diagnosis in dynamic systems using analytical and knowledge-based redundancy - a survey and some new results. *Automatica*, 26:459–474, 1990.

[10] P. Goupil. Airbus state of the art and practices on fdi and ftc. In *Proceedings of Safeprocess'09*, 2009.

[11] Philippe Goupil. Oscillatory failure case detection in the a380 electrical flight control system by analytical redundancy. *Control Engineering Practice*, 18:1110–1119, 2009.

[12] Simon Hecker. *Generation of low order LFT Representations for Robust Control Applications*. Dissertation, Technische Universitt Mnchen, Mnchen, 2006.

[13] Thuan H. Khong and Jong-Yeob Shin. Robustness analysis of integrated lpv-fdi filters and lti-ftc system for a transport aircraft. In *AIAA Guidance, Navigation and Control Conference and Exhibit*, 2007.

[14] M.A. Massoumnia. A geometric approach to the synthesys of failure detection filters. *IEEE Transactions on Automatic Control*, 31:839–846, 1986.

[15] M.A. Massoumnia, G.C. Verghese, and A.S. Willsky. Failure detection and identification. *IEEE Transactions on Automatic Control*, 34:316–321, 1989.

[16] R. J. Patton and J. Chen. Robust fault detection and isolation FDI systems. *Contr. Dynamic Syst.*, 74:176–224, 1996.

[17] P. Seiler, B. Vanek, J. Bokor, and G.J. Balas. Robust H_∞ filter design using frequency gridding. In *Submitted to the 2011 American Control Conference*, 2011.

[18] Robert F. Stengel. *Flight Dynamics*. Princeton University Press, 2004.

[19] I. Szaszi, A. Marcos, G.J. Balas, and J. Bokor. LPV detection filter design for a Boeing 747-100/200 aircraft. *AIAA Journal of Guidance, Dynamics and Control*, 28(3):461–470, 2005.

[20] D. Van den Bossche. The a380 flight control electrohydrostatic actuators, achievements and lessons learnt. In *Proc. 25th Congress of the International Council of the Aeronautical Sciences*, 2006.

[21] B. Vanek, P. Seiler, J. Bokor, and G.J. Balas. Robust fault detection filter design for commercial aircraft. In *Euro GNC 2011 1st CEAS Specialist Conference on Guidance, Navigation & Control, Münich*, 2011.

[22] A. Varga. On computing least order fault detectors using rational nullspace bases. In *In Proceedings of the IFAC Symp. SAFEPROCESS'2003, Washington D.C.*, 2003.